Molecular Dynamics

DOI: 10.1002/ange.200601778

Ultrafast Electron Crystallography of Phospholipids**

*Songye Chen, Marco T. Seidel, and Ahmed H. Zewail**

We report herein our first study on the structure and dynamics of mono- and bilayer phospholipids, the essential elements of biological membranes, by using ultrafast electron crystallography (UEC).[1,2] The phospholipid was immobilized as a Langmuir–Blodgett film on hydrophilic or hydrophobic silicon substrates. From the diffraction patterns we determined that the dimyristoyl phosphatidic acid (DMPA; Figure 1) molecules were aligned with their aliphatic chains perpendicular to the substrate surface, and resolved the subunit cell -CH_2-CH_2-CH_2- distance to be $c_0 = 2.54$ Å. After a femtosecond temperature jump in the substrate we observed, through changes in the position and intensity of the diffraction, structural dynamics on different time scales: a coherent, non-equilibrium expansion (wave-type) along the aliphatic chains on the picosecond timescale, as well as contraction and restructuring at longer times. Moreover, transient structural ordering was revealed on the ultrashort time scale. For this complex system, UEC allowed us to picture the atomic forces involved in structural dynamics at far-from-equilibrium configurations, whose collective and coherent effects may otherwise be obscured.

The resemblance of both lipid Langmuir films at water surfaces and Langmuir–Blodgett (LB) films to naturally occurring biological membranes means they often serve as model systems for studying membrane structures and properties,[3,4] such as head-group organization and hydration,[5] phase transitions,[6] interactions with membrane proteins,[7,8] and proton diffusion,[9] besides other applications in molecular electronics[10] and biological sensors.[11] Studies on the structure of lipid LB films have mostly been focused on fatty acids and fatty acid salts,[12] but for phospholipids, although more complex and less studied, their structures have been probed by a variety of techniques, including electron diffraction,[13–15] X-ray diffraction,[5,16] infrared spectroscopy,[17,18] scanning tunneling microscopy,[19] and atomic force microscopy.[20]

Structural ultrafast dynamics have not been reported. Ultrafast optical spectroscopy has been used to probe the dynamics of water solvation,[21] and inelastic neutron scattering has enabled the deduction of time scales of collective motions from the dispersion relationships.[22] UEC is well suited for the study of structural changes because of its high sensitivity, low damage at low electron flux,[23] and spatiotemporal resolutions. All experiments were carried out in our UEC apparatus,[2,24] in which the electrons are incident at a grazing angle of $\theta_i = 0$–$5°$ and are scattered by the lipid molecules to form the diffraction patterns in the far field. The scattered electrons are recorded with a low-noise, image-intensified, charge-coupled device (CCD) camera assembly capable of single-electron detection.[23]

The change of the structure was initiated by a femtosecond infrared laser pulse (800 nm, 120 fs, 1 kHz repetition rate) focused onto the sample surface at an incidence angle of 30° and an area of illumination of approximately 1.3 mm^2. Part of this IR beam was frequency tripled (266 nm, ca. 10 nJ) and used to synchronously generate the ultrashort electron pulses (30 keV, $\lambda_{\text{de Broglie}} = 0.07$ Å) through the photoelectric effect. A series of diffraction frames were recorded at a specified time delay by adjusting the time delay between the laser and electron pulses. When combined, these frames give the real-time change of the structure. The time zero was determined in situ.

The lipids are deposited (see Experimental Section) in the so-called Y geometry, that is, head-to-head and tail-to-tail. In the case of a hydrophilic substrate, the first layer is attached to the surface by its hydrophilic head, while for a hydrophobic substrate the attachment is through the hydrophobic tail (see Figure 1B). We used a hydrophilic oxide-terminated silicon-(111) surface for deposition of the monolayer, and a hydrophobic hydrogen-terminated silicon(111) surface for the bilayer (See Experimental Section). Isotherms of the Langmuir film and the transfer ratio at deposition were recorded to ensure the LB films were of high quality. The morphology of

[*] S. Chen, Dr. M. T. Seidel, Prof. Dr. A. H. Zewail
Laboratory for Molecular Sciences, and
Physical Biology Center for Ultrafast Science and Technology
California Institute of Technology
Pasadena, CA 91125 (USA)
Fax: (+1) 626-792-8456
E-mail: zewail@caltech.edu

[**] This work was supported by the National Science Foundation. We thank Prof. J. Heath for the use of his LB facility, E. DeIonno, J.-W. Choi, P. Cao, Dr. Y. Luo, and Dr. H. Yu for advice and discussion on LB films, and the three referees for helpful suggestions.

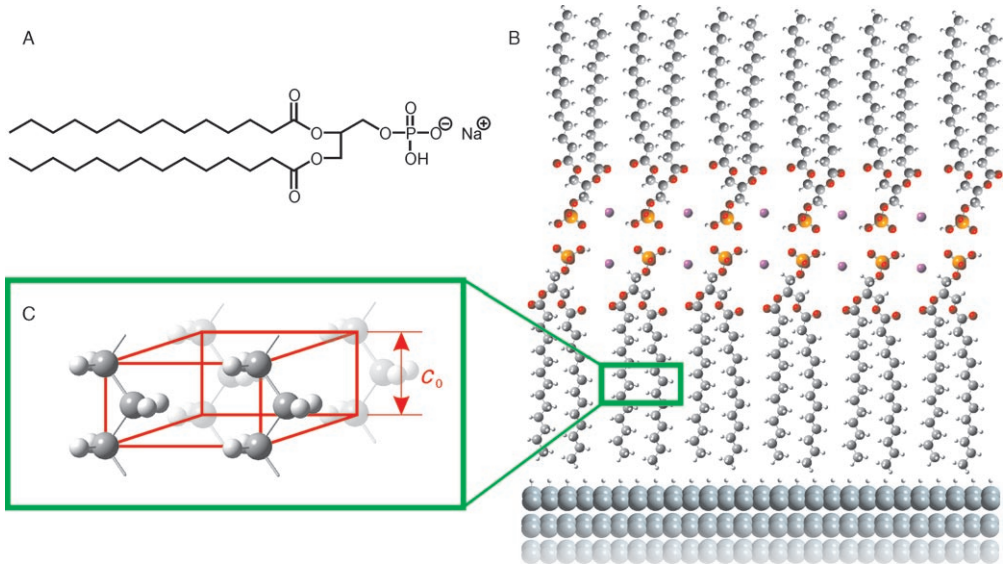

Figure 1. A) A view of the molecular structure, B) the phospholipid DMPA on the substrate, and C) the C_2H_4 subunit cell, with the distance c_0 between the CH_2 groups shown.

the lipids at the air–water interface was monitored with a Brewster angle microscope and no holes or multilayer islands were found. The samples were transferred immediately after deposition into an ultrahigh vacuum (UHV, ca. 10^{-10} Torr), in which all the experiments were carried out. The LB films are stable to electron exposure, as evidenced by the absence of deterioration in the quality of the static diffraction patterns. For a typical pulse of 10^3 electrons at our repetition rate the dosage level is about 10^{-6} electrons s^{-1} Å^{-2}, and for exposure over several hours this translates to about 10^{-2}–10^{-1} electrons Å^{-2}. It is also significant to note that the dosage is provided in a pulsed mode with sufficient time (1 ms) to dissipate the heat.

The electron diffraction recorded here is mainly sensitive to the C_2H_4 subunit of the aliphatic chains[25] as a consequence of the s range covered, where s is the momentum transfer between the incident electron and the scattered electron, that is, $s = kR/L$; $k = 1/\lambda_{\text{de Broglie}}$, R is the distance between a diffraction spot and the main beam position on the screen, and L is the distance between the sample and the screen. The molecular structure of DMPA (Figure 1 A) is similar to that of fatty acids, but with some differences: there are two aliphatic chains instead of one, and there is a different head group. Phospholipids organize in a two-dimensional hexagonal lattice where the aliphatic chains pack parallel to each other and perpendicular to the surface.[13–15,17,18] The structure of the C_2H_4 subunit cell is illustrated in Figure 1 C.

The static diffraction patterns of the monolayers and bilayers (Figure 2 B and C, respectively) are similar. The strongest feature of the patterns is the horizontal (or slightly curved) line, which is labeled by the Miller indices ($hk2$). The diffraction line is basically the composite of Bragg diffractions

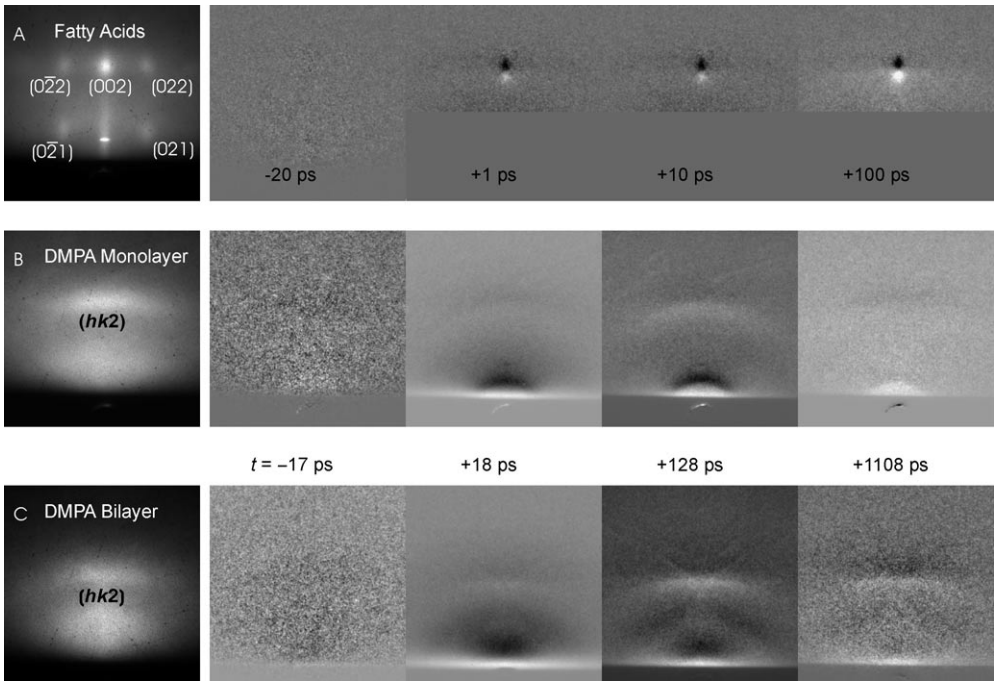

Figure 2. The static diffraction patterns and the diffraction difference patterns of DMPA monolayers, bilayers, and fatty acids on substrates. The diffraction difference patterns of the fatty acid (arachidic acid calcium salt) bilayer are shown with the time delays indicated. For the DMPA molayers and bilayers, the Bragg spots appear as lines on a diffuse background. We note that the diffraction difference patterns at negative times show no features, as expected.

(see Panel A for the fatty acids). The subunit cell parameter c_0 was determined from the s value in the vertical direction to be 2.54 Å, which is representative of the -CH_2-CH_2-CH_2- distances, as shown in Figure 1 C. This distance is nearly the same as that determined for the LB films of fatty acids (Figure 2 A). The diffraction line pattern indicates that, although the LB films consist of many crystalline domains, the aliphatic chains are packed parallel to each other. The fact that the diffraction line is oriented parallel to the shadow edge means that the aliphatic chains are aligned nearly perpendicular to the surface. The diffraction patterns in the lower s range show diffuse scattering from the different crystalline domains. The diffraction pattern was independent of the electron incidence angle θ_i and the azimuthal angle ϕ, which is consistent with the presence of polycrystalline domains.

The diffraction patterns change significantly following the heating of the substrate with an ultrafast IR laser pulse. This is shown in the frame difference patterns in Figure 2 B and C for the monolayers and bilayers, respectively. Before time zero, that is, when the electron pulse arrives prior to the heating pulse, the diffraction difference patterns are featureless (shown in Figure 2 B and C for $t = -17$ ps). After time zero, the patterns show a change in the ($hk2$) line position—becoming dark at the higher s value and bright at the lower s value, which indicates a downward movement of the line with time. Shrinkage in the reciprocal space corresponds to an expansion in real space. Therefore, the downward movement of the diffraction line means an increase of the -CH_2-CH_2-CH_2- distances along the aliphatic chains.

To quantify the change in the structure with time, we fitted the ($hk2$) diffraction line in the vertical s direction with a Voigt function, thus providing the exact peak center position and integrated intensity at each time point. From the center position, the subunit cell parameter c_0 was obtained, and its change as a function of time is shown in Figure 3 A and B for monolayers and bilayers, respectively. The dynamics of the change is similar for both samples, showing a successive increase in the c_0 value (total ca. 50 ps) and the recovery back (ca. 500 ps) on our time scale. However, the amplitude of the expansion in the monolayer is smaller than in the bilayer by nearly a factor of three. Similar behavior was also observed for fatty acids studied as a function of thickness.[25,26]

For ordered materials we expect the transient intensity change to follow that of the shift Δc_0. By integrating over the vertical s range, after careful removal of the background, we obtained the results depicted in Figure 3. The intensity initially drops within about 15 ps after heating with the IR laser, but then increases to even above the static value in approximately 130 ps, and finally recovers back to the initial value at longer times (ca. 400 ps). The initial drop in the intensity is consistent with the disorder induced by the heating pulse. This disorder is typically described by the thermal (incoherent) motion of atoms and can be expressed using standard Debye–Waller factors. However, the subsequent increase in the intensity above the static value indicates the formation of a more-ordered state on the ultrafast time scale and is certainly nonthermal. Comparing the shift and the intensity change with time, we see that when the elongation reaches its maximum, the intensity (toward order) is also at its highest, but the intensity maximum toward disorder occurs at a shorter time. At longer times, the behavior becomes comparable. Similar trends in the intensity behavior were

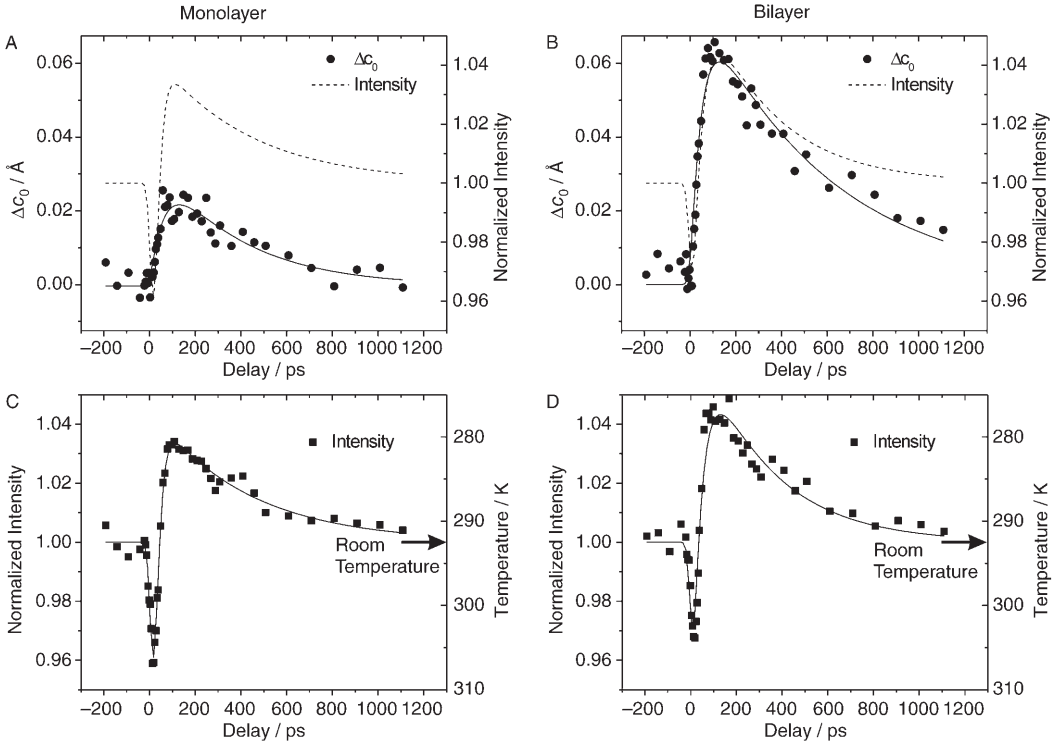

Figure 3. Dynamics of structural change. The axial change Δc_0 and the normalized intensity of the ($hk2$) diffraction line as a function of time for: A) and C) the monolayer, and B) and D) the bilayer of the phospholipid.

observed for the fatty acids.[26] The width of the diffraction line contains information on changes in the order/disorder of fatty acids, but for phospholipids the signal-to-noise ratio was not sufficiently high to ascertain the significance of the change. We have measured the change in intensity with temperature under steady-state conditions for fatty acids, and if such a change is similar to that of the phospholipids, then the temperature scale in Figure 3C and D would reflect the corresponding equilibrium values. In the simplest model of harmonic chains, a change of 0.02 Å corresponds to a temperature increase of approximately 30 K, in the non-equilibrium regime.

The net change in displacement is determined by the impulsive force (temperature) of the substrate (including coupling) and the maximum value of the extension depends on the elasticity and heat capacity. If heating occurs for an equilibrated system, the change in the value of c_0 with temperature Δc_0 should be independent of the number of C-C-C subunits in the chain, and $\Delta c_0/c_0$ becomes simply α (the thermal expansion coefficient), which is typically very small (10^{-4}–10^{-6}).[27] However, for non-equilibrium dynamics, the impulsive force at short times transmit a large change in the value of Δc_0 as the disturbance (wave-type) accumulates to give the net effect that is dependent on the number of C atoms.[28] Both the observed amplitude of the change and the rise in time are consistent with this non-equilibrium wave-type propagation at ultrashort time and equilibration at much longer times. This picture also explains the dependence on the total length of the chains. Quantification of the total change must take into account the variation in the density of the LB films upon going from single to multiple layers and the nature of the substrate force. It is known that "defects" or holes can be formed when multiple layers are deposited.[29] Moreover, as the effect of the substrate decreases with increasing distance (in this case chain length), some disorder is expected.[30]

The fact that the initial change in intensity (and elongation) occurs within 15 ps and that the distance traveled is approximately 20 Å (for a monolayer) predicts a speed of propagation that is sub-kilometers per second, which is close to the propagation of sound waves (underdamped regime); future experiments will examine this region at different times and temperatures. It will be shown elsewhere[28] that the frequencies of C-C-C motion and force in the diffusive (overdamped) regime have to be unrealistically large. In the underdamped regime, although the force is significant to cause the large change in Δc_0, and coherent propagation is within the chain, the change in the value of Δc_0 relative to that of c_0 is relatively small to preserve the robustness of the Bragg spots throughout the temporal change. However, it is important to point out that for large complex systems the diffraction has features of both "crystalline" and "diffusive" scatterings. The latter gives structural information on the collective motions, which can be examined through cross-terms of Debye–Waller factors.[31] In this regard, the ring(s) apparent at $s \approx 0.3$ Å^{-1} in the diffraction difference patterns should be analyzed for such correlations in the phospholipid, and we shall consider this analysis elsewhere.

The structural dynamics can now be pictured. Since the phospholipids have no resonance absorption at 800 nm, which is the wavelength of the heating IR laser pulse, the energy is absorbed by the substrate. The energy is transferred within a few picoseconds into the substrate lattice (through electron–phonon coupling), which results in an expansion of the substrate lattice.[24,25] On this time scale, the energy is transferred to the adsorbate, where it flows along the aliphatic chains of the DMPA molecules through vibrational motion. The net effect is the elongation of the C_2H_4 subunits. This transport of heat at an early time first induces transient disorder, which causes the intensity of the (*hk*2) diffraction line to drop in the first 15 ps. This result is expected in a Debye–Waller picture, as the degree of inhomogenity along the chains increases with temperature. However, with time, the lipids enter a more ordered state, which manifests itself in an increased diffraction intensity even above the initial value. This effect is achieved by overcoming some energy barrier and through alignment of the aliphatic chains by rotation and other motions, and possibly through transient annealing of the film, which because of defects could have more effect in multiple layers than monolayers. This enhanced structural ordering may be common, even in self-assembly, but it can only be observed[32] in the non-equilibrium state at short times. When the energy dissipates into the substrate, the aliphatic chains of the DMPA molecules begin to contract and restructure toward the initial equilibrium state on the nanosecond time scale. It is known that different phases ("gel" and "liquid") do exist depending on the temperature, and it is interesting that neutron scattering studies give a lifetime of 17 ps for the acoustic phonon excitation in the gel phase.[22]

In conclusion, it has been demonstrated here that monolayer and bilayer phospholipids on hydrophilic and hydrophobic substrates can be studied using UEC. The combined structures (unit cell and orientation) and dynamics (after femtosecond laser heating) are reported, thus providing insights into the nature of atomic motions and energy transfer—coherent versus diffusive—in phospholipids. The transient structural ordering discussed here may be significant to dynamic assembly and collective motions (which occur at short times) in bilayers and possibly membranes. Future work will consider the role of hydration.

Experimental Section

1,2-Dimyristoyl-*sn*-glycero-3-phosphate monosodium salt (dimyristoyl phosphatidic acid, DMPA) was purchased from Aldrich and used without further purification. The lipids were spread from a chloroform/methanol (3:1) solution, and the subphase used was Millipore water containing sodium ions at pH 5.5. The deposition took place in an NIMA Langmuir–Blodgett dipping trough at a dipping pressure of $\pi = 29$ mN m^{-1} and a dipping speed of 1 mm min^{-1}.

Hydrophilic silicon surfaces were prepared just before deposition by cleaning and oxidation with an RCA-1 solution. For the hydrophobic surfaces, subsequent etching of the oxide surface was made in a 40% NH_4F solution for 15–20 min to give the Si(111):H surface.

Received: May 5, 2006

Keywords: diffraction · Langmuir–Blodgett films · molecular dynamics · phospholipids · surface assembly

[1] J. M. Thomas, *Angew. Chem.* **2004**, *116*, 2658; *Angew. Chem. Int. Ed.* **2004**, *43*, 2606.
[2] F. Vigliotti, S. Chen, C.-Y. Ruan, V. A. Lobastov, A. H. Zewail, *Angew. Chem.* **2004**, *116*, 2759; *Angew. Chem. Int. Ed.* **2004**, *43*, 2705.
[3] G. Roberts, *Langmuir-Blodgett Films*, Plenum, New York, **1990**.
[4] M. C. Petty, *Langmuir-Blodgett Films*, Cambridge University Press, Cambridge, **1996**.
[5] M. Dyck, P. Krüger, M. Lösche, *Phys. Chem. Chem. Phys.* **2005**, *7*, 150.
[6] C. A. Helm, P. Tippmann-Krayer, H. Möhwald, J. Alsnielsen, K. Kjaer, *Biophys. J.* **1991**, *60*, 1457.
[7] I. Fujiwara, M. Ohnishi, J. Seto, *Langmuir* **1992**, *8*, 2219.
[8] M. Subirade, C. Salesse, D. Marion, M. Pezolet, *Biophys. J.* **1995**, *69*, 974.
[9] J. Zhang, P. R. Unwin, *J. Am. Chem. Soc.* **2002**, *124*, 2379.
[10] K. Norgaard, T. Bjornholm, *Chem. Commun.* **2005**, 1812.
[11] A. P. Girard-Egrot, S. Godoy, L. J. Blum, *Adv. Colloid Interface Sci.* **2005**, *116*, 205.
[12] D. K. Schwartz, *Surf. Sci. Rep.* **1997**, *27*, 241.
[13] S. W. Hui, D. F. Parsons, M. Cowden, *Proc. Natl. Acad. Sci. USA* **1974**, *71*, 5068.
[14] L. L. Orekhova, A. Mogilevich, S. V. Orechov, V. V. Klechkovskaya, L. A. Feigin, *Phys. B* **1994**, *198*, 144.
[15] M. Stevens, M. Longo, D. L. Dorset, J. Spence, *Ultramicroscopy* **2002**, *90*, 265.
[16] M. Seul, P. Eisenberger, H. M. McConnell, *Proc. Natl. Acad. Sci. USA* **1983**, *80*, 5795.
[17] B. W. Gregory, R. A. Dluhy, L. A. Bottomley, *J. Phys. Chem.* **1994**, *98*, 1010.
[18] P. Lozano, A. J. Fernández, J. J. Ruiz, L. Camacho, M. T. Martín, E. Muñoz, *J. Phys. Chem. B* **2002**, *106*, 6507.
[19] J. K. H. Hörber, C. A. Lang, T. W. Hänsch, W. M. Heckl, H. Möhwald, *Chem. Phys. Lett.* **1988**, *145*, 151.
[20] J. M. Solletti, M. Botreau, F. Sommer, W. L. Brunat, S. Kasas, T. M. Duc, M. R. Celio, *Langmuir* **1996**, *12*, 5379.
[21] H. Bürsing, D. Ouw, S. Kundu, P. Vöhringer, *Phys. Chem. Chem. Phys.* **2001**, *3*, 2378.
[22] M. C. Rheinstadter, C. Ollinger, G. Fragneto, F. Demmel, T. Salditt, *Phys. Rev. Lett.* **2004**, *93*, 108107.
[23] R. Srinivasan, V. A. Lobastov, C.-Y. Ruan, A. H. Zewail, *Helv. Chim. Acta* **2003**, *86*, 1761.
[24] C.-Y. Ruan, F. Vigliotti, V. A. Lobastov, S. Chen, A. H. Zewail, *Proc. Natl. Acad. Sci. USA* **2004**, *101*, 1123.
[25] S. Chen, M. T. Seidel, A. H. Zewail, *Proc. Natl. Acad. Sci. USA* **2005**, *102*, 8854.
[26] M. T. Seidel, S. Chen, A. H. Zewail, unpublished results.
[27] T. Fukui, M. Sugi, S. Iizima, *Phys. Rev. B* **1980**, *22*, 4898.
[28] J. Tang, A. H. Zewail, unpublished results.
[29] J. B. Peng, G. T. Barnes, I. R. Gentle, *Adv. Colloid Interface Sci.* **2001**, *91*, 163.
[30] C.-Y. Ruan, V. A. Lobastov, F. Vigliotti, S. Chen, A. H. Zewail, *Science* **2004**, *304*, 80.
[31] L. Meinhold, J. C. Smith, *Phys. Rev. Lett.* **2005**, *95*, 218103.
[32] C.-Y. Ruan, D.-S. Yang, A. H. Zewail, *J. Am. Chem. Soc.* **2004**, *126*, 12797.

